THE ASTROPHYSICAL JOURNAL, 263:791–802, 1982 December 15

EVOLUTION OF CHROMOSPHERES AND CORONAE IN SOLAR MASS STARS: A FAR-ULTRAVIOLET AND SOFT X-RAY COMPARISON OF ARCTURUS (K2 III) AND ALPHA CENTAURI A (G2 V)

THOMAS R. AYRES[1,2]
Laboratory for Atmospheric and Space Physics, University of Colorado
THEODORE SIMON[1]
Institute for Astronomy, University of Hawaii
AND
JEFFREY L. LINSKY[1,2,3]
Joint Institute for Laboratory Astrophysics, National Bureau of Standards and University of Colorado
Received 1982 April 5; accepted 1982 June 18

ABSTRACT

We compare *IUE* far-ultraviolet and *Einstein* soft X-ray observations of the red giant Arcturus (α Boötis, K2 III) and the nearby yellow dwarf α Centauri A (G2 V), which are archetypes of solar mass stars in very different stages of evolution. We find no evidence for coronal ($T \approx 10^6$ K) soft X-ray emission from the red giant at surface flux levels of only 0.0006 (3σ) that detected previously for α Cen A, and no evidence for C IV $\lambda\lambda$1548, 1551 ($T \approx 10^5$ K) or C II $\lambda\lambda$1335, 1336 ($T \approx 2 \times 10^4$ K) resonance line emission at surface flux levels of only 0.02 (3σ) those of the yellow dwarf. Instead of a solar-like hot corona and warm ($T \approx 10^5$ K) transition region, the resonance line upper limits and previous detections of the C II *intersystem* UV multiplet 0.01 near 2325 Å provide evidence that the outer atmosphere of Arcturus is geometrically extended ($\Delta h \sim R_*$), tenuous ($n_e \approx 3 \times 10^8$ cm^{-3}), and cool ($T \lesssim 10^4$ K).

A second important difference between Arcturus and α Cen A is the prominent cool stellar wind of the red giant. The terminal velocity inferred from the blueshifted absorption components in the O I and Mg II resonance lines is $v_\infty = 40$–50 km s^{-1}, the estimated mass loss rate is $\gtrsim 3 \times 10^{-10}$ $M_\odot$ yr^{-1}, and the angular momentum loss is at least four orders of magnitude larger than that of the weak coronal wind of the Sun. The rapid spin-down of a post–main-sequence solar mass star, owing initially to evolutionary expansion and later to the development of a strong wind, is likely to severely inhibit the generation and amplification of magnetic fields by the dynamo mechanism. The decline in magnetic activity with evolution into the giant branch may account for the extraordinary weakness of Arcturus in X-rays compared with α Cen A, since hot coronae are likely to be associated with strong surface magnetic fields.

Finally, we provide an extensive tabulation of line identifications, widths, and fluxes for the *IUE* far-ultraviolet echelle spectra of the two stars; we discuss the two competing explanations for the Wilson-Bappu effect; and we illustrate the "missing line" phenomenon in the Arcturus high-dispersion spectrum, which quite likely is produced by fluoresced carbon monoxide bands.

Subject headings: stars: chromospheres — stars: coronae — stars: individual (α Boo, α Cen A) — stars: winds — ultraviolet: spectra — X-rays: sources

I. INTRODUCTION

A number of studies have demonstrated that single dwarf stars suffer a general decay of their chromospheric ($T \approx 6 \times 10^3$ K) Ca II H and K emission with increasing age on the main sequence (cf. Wilson 1963). Quantitatively, the surface flux of Ca II emission appears to decline as the square root of age, $F_{\text{Ca II}} \sim t^{-0.5}$ (Skumanich 1972; Duncan 1981). More recently, far-ultraviolet and soft X-ray surveys of solar type stars in young and intermediate-age clusters have revealed that emission from higher temperature layers of the stellar outer atmosphere analogous to the solar transition region (TR: $T \approx 10^5$ K) and corona ($T \gtrsim 10^6$ K) declines with increasing age at a faster rate than the chromospheric Ca II emission. For example, C IV ($T \approx 10^5$ K) surface fluxes decay as $t^{-0.9}$ (Boesgaard and Simon 1981), and 1/4 keV soft X-ray ($\gtrsim 10^6$ K) surface fluxes

[1]Guest observer, *International Ultraviolet Explorer*.
[2]Guest observer, *Einstein X-ray Observatory*.
[3]Staff member, Quantum Physics Division, National Bureau of Standards.

decrease roughly as $t^{-1.3}$ (Stern *et al.* 1981; Caillault, Helfand, and Ku 1981). Since chromospheric and coronal emission on the Sun is strongly associated with surface magnetic fields (e.g., Skumanich, Smythe, and Frazier 1975; Withbroe and Noyes 1977; Vaiana and Rosner 1978), the fading of Ca II, C IV, and soft X-ray brightness among the older dwarfs very likely indicates a decline in their magnetic activity. A promising mechanism is the weakening of dynamo action (Parker 1970) with the slow spin-down of the star driven by the angular momentum loss in a mild coronal wind (Durney 1972).

One expects, however, a much more rapid spin-down as a star evolves away from the main sequence, owing to the substantial expansion of the stellar outer envelope during shell hydrogen burning. Furthermore, the dramatic change in stellar properties as a dwarf becomes a giant should affect the ways in which magnetic activity is expressed *structurally* on the stellar surface. For example, the giants redward of a nearly vertical boundary in the H-R diagram near color index $(V-R)=0.8$ typically exhibit the spectroscopic signatures of substantial mass loss in cool, slow stellar winds unlike the tenuous, hot, high-speed coronal wind of the Sun (Stencel and Mullan 1980). These same red giants typically exhibit little or no emission in sensitive indicators of high-temperature plasma, such as C IV and soft X-rays (see Linsky and Haisch 1979; Ayres, Marstad, and Linsky 1981; Ayres *et al.* 1981; Simon, Linsky, and Stencel 1982).

Here, we examine the fate of the chromosphere and corona, and by implication the stellar surface magnetic field, as evolution greatly alters the physical characteristics of a solar mass star. In particular, we compare far-ultraviolet and soft X-ray measurements of the archetype red giant Arcturus (α Boo; K2 III) and a stellar twin of the Sun, α Cen A (G2 V), obtained with the *International Ultraviolet Explorer* (*IUE*; Boggess *et al.* 1978) and the *Einstein X-ray Observatory* (Giacconi *et al.* 1979).

II. OBSERVATIONS

a) Selection Criteria

Several considerations motivated our choice of Arcturus and α Cen A for this study. First, the high space velocity, mild metal deficiency, and low spectroscopic surface gravity of Arcturus imply that it is old chronologically (perhaps 10^{10} yr), and very likely has evolved from a $\gtrsim 1\ M_{\odot}$ progenitor not too different from α Cen A or the Sun (see Griffin and Griffin 1967). Therefore, Arcturus provides a reliable benchmark for the future evolution of a solar mass star. Second, fundamental stellar parameters such as radii, luminosities, masses, and effective temperatures are known fairly reliably for both stars (cf. Mäckle *et al.* 1975; Ayres and Johnson 1977; Flannery and Ayres 1978). Third, because Arcturus is the brightest of the nearby red giants, and α Cen A is the brightest of the yellow dwarfs, we can compare the outer atmosphere phenomena of the two archetypes with the highest sensitivity. Finally, we utilize α Cen A as a representative solar mass dwarf because neither *IUE* nor *Einstein* can observe the Sun, itself, directly. We summarize adopted stellar parameters for Arcturus and α Cen A in Table 1, and the circumstances of our *IUE* and *Einstein* observations in Table 2.

TABLE 1

ADOPTED STELLAR PARAMETERS

Parameter	α Boötis[a]	α Centauri A[b]
Spectral type	K2 III	G2 V
d (pc)	10.9	1.34
V (mag)	−0.05	−0.01
$V-R$ (mag)	+0.97[c]	(+0.53)[d]
l_{bol} (10^{-5} ergs cm^{-2} s^{-1})[e]	4.9	2.7
ϕ' (10^{-3} arcsec)[f]	21.4	8.8
F_L/f_L[g]	3.7×10^{14}	2.2×10^{15}
$R/R_{\odot}$[h]	25	1.3
$L/L_{\odot}$[i]	180	1.5
T_{eff} (K)[j]	4225	5675
$M/M_{\odot}$	1.1[k]	1.1

[a] From Mäckle *et al.* 1975, unless otherwise indicated.
[b] From Flannery and Ayres 1978, unless otherwise indicated.
[c] Johnson *et al.* 1966.
[d] Thomas, Hyland, and Robinson 1973.
[e] Ayres, Marstad, and Linsky 1981.
[f] Stellar angular diameter: see Linsky *et al.* 1979.
[g] Conversion from apparent flux to surface flux.
[h] $R/R_{\odot}=0.108\phi' d$.
[i] $L/L_{\odot}=0.313 l_{bol} d^2$.
[j] $T_{eff}=13133 l_{bol}^{1/4}(\phi')^{-1/2}$.
[k] Ayres and Johnson 1977.

b) Einstein Observations

The *Einstein Observatory* obtained a 12,950 s (216 minute) High Resolution Imager (HRI) observation of Arcturus on 1981 January 23. The effective exposure time near the center of the HRI field was 11,800 s. No source was detected at the position of Arcturus to a limiting 3 σ count rate of 0.0005 counts s^{-1}. For a solar-temperature corona ($T\approx 2\times10^6$ K), the upper limit corresponds to a flux of less than 2×10^{-14} ergs cm^{-2} s^{-1} at Earth (see Golub *et al.* 1982).

In contrast, Golub *et al.* (1982) detected α Cen A with the HRI at a level of 0.140 counts s^{-1}, corresponding to a flux of 6×10^{-12} ergs cm^{-2} s^{-1} at Earth. The inferred X-ray luminosity of α Cen A, $L_x=1.2\times10^{27}$ ergs s^{-1}, is quite similar to that of the Sun at the minimum of its activity cycle (Golub *et al.* 1982).

The sensitivity of the HRI to coronal emission falls rapidly for sources cooler than 10^6 K. Consequently, we

TABLE 2

OBSERVATIONS

Target	Image Number[a]	JD (mid-exposure) 2,443,000+	Exposure Time (minutes)
α Boötis	H 10290	1628.01	216
	SWP 11039	1617.34	420
	LWR 9703	1617.82	3
α Centauri A ...	H 940[b]	1118.57	18
	SWP 5541[c]	1040.92	120
	SWP 11017	1615.34	400
	LWR 2093	737.66	2
	LWR 2094	737.71	1

[a] H = *Einstein* X-ray Observatory; High Resolution Imager (0.1–4 keV). SWP, LWR = *International Ultraviolet Explorer* echelle exposure through large aperture (10″×20″); 1150–2000 Å, 2000–3000 Å regions, respectively.

[b] See Golub *et al.* 1982.

[c] See Ayres *et al.* 1982. Effective exposure time 109 minutes, because star was positioned near edge of large aperture to displace geocoronal Lyα feature longward of interstellar D I absorption feature.

cannot set meaningful limits on the presence of a "warm" ($T = \text{few} \times 10^5$ K) corona on the basis of the *Einstein* HRI image. However, several prominent resonance lines of 10^5 K plasma fall within the *IUE* far-ultraviolet (1150–2000 Å) bandpass, and observations of these features can constrain the amount of warm material that might be present in the outer atmosphere of Arcturus.

c) *IUE Observations*

On 1981 January 12, less than two weeks prior to the *Einstein* observation, we obtained a 420 minute high-dispersion spectrum of Arcturus with the far-ultraviolet echelle spectrograph of *IUE*. We also took a 3 minute exposure of the middle-ultraviolet region (2000–3000 Å) with the long wavelength echelle. On 1981 January 10, we obtained a 400 minute far-ultraviolet echelle spectrum of α Cen A to supplement a series of shorter (2 hr) exposures analyzed in an earlier study (Ayres *et al.* 1982). Long-wavelength exposures of α Cen A also are available from a previous study (Ayres and Linsky 1980).

We reduced the echelle spectra in the manner described by Ayres *et al.* (1982), although we have replaced the "1 σ" interorder background filter used in that study with a 100-point running mean. We have placed the spectra on an absolute flux scale by means of the provisional echelle-mode calibration for sharp-line emission sources proposed by Cassatella, Ponz, and Selvelli (1981). Furthermore, we have subjected the H I λ1216 (Lyα) and the Mg II λ2796 (*k*) and λ2803 (*h*) resonance lines to an "active" blaze correction that iteratively adjusts the echelle grating constant to balance a prespecified bandpass common to the adjacent orders in which the respective features repeat. We registered the velocity scale of each SWP image according to the laboratory wavelengths of about 10 sharp, isolated emission features distributed across the echelle format. We established rest frame velocities for the H I and Mg II resonance lines by fitting least-squares Gaussians to the outermost portions of the emission cores which are not affected by interstellar or circumstellar absorption.

Figure 1 compares the far-ultraviolet emission spectra of Arcturus and α Cen A. The brightest features of the latter—Lyα and the Si II 1815 Å triplet—are from the 120 minute observation (see Table 2) since those regions are saturated in the 400 minute exposure. Table 3 provides a comparison of fluxes and profile shape parameters, measured by least-squares Gaussian fits to the prominent lines of each spectrum. For several regions of the Arcturus spectrum, we determined 3 σ upper limits for unseen lines based on the rms fluctuation level at the expected wavelength and the FWHM of the observed feature in the α Cen A spectrum.

Figure 2 depicts the Mg II regions of α Cen A and Arcturus. Comparisons of *h* and *k* line strengths and profile parameters are included in Table 3.

III. DISCUSSION

a) *Weakness of High-Temperature Emission from Arcturus*

By any measure, the upper limit on soft X-ray emission from Arcturus is considerably smaller than the observed flux from α Cen A. The volume emission measure, $\int n_e^2\, dV$ (or total luminosity, L_x), of multimillion degree plasma in the outer atmosphere of Arcturus is at least a factor of 3 smaller than that of α Cen A, which itself has a rather inactive corona like the Sun. Furthermore, Arcturus is a factor of about 500 weaker than α Cen A in the X-ray-to-bolometric flux

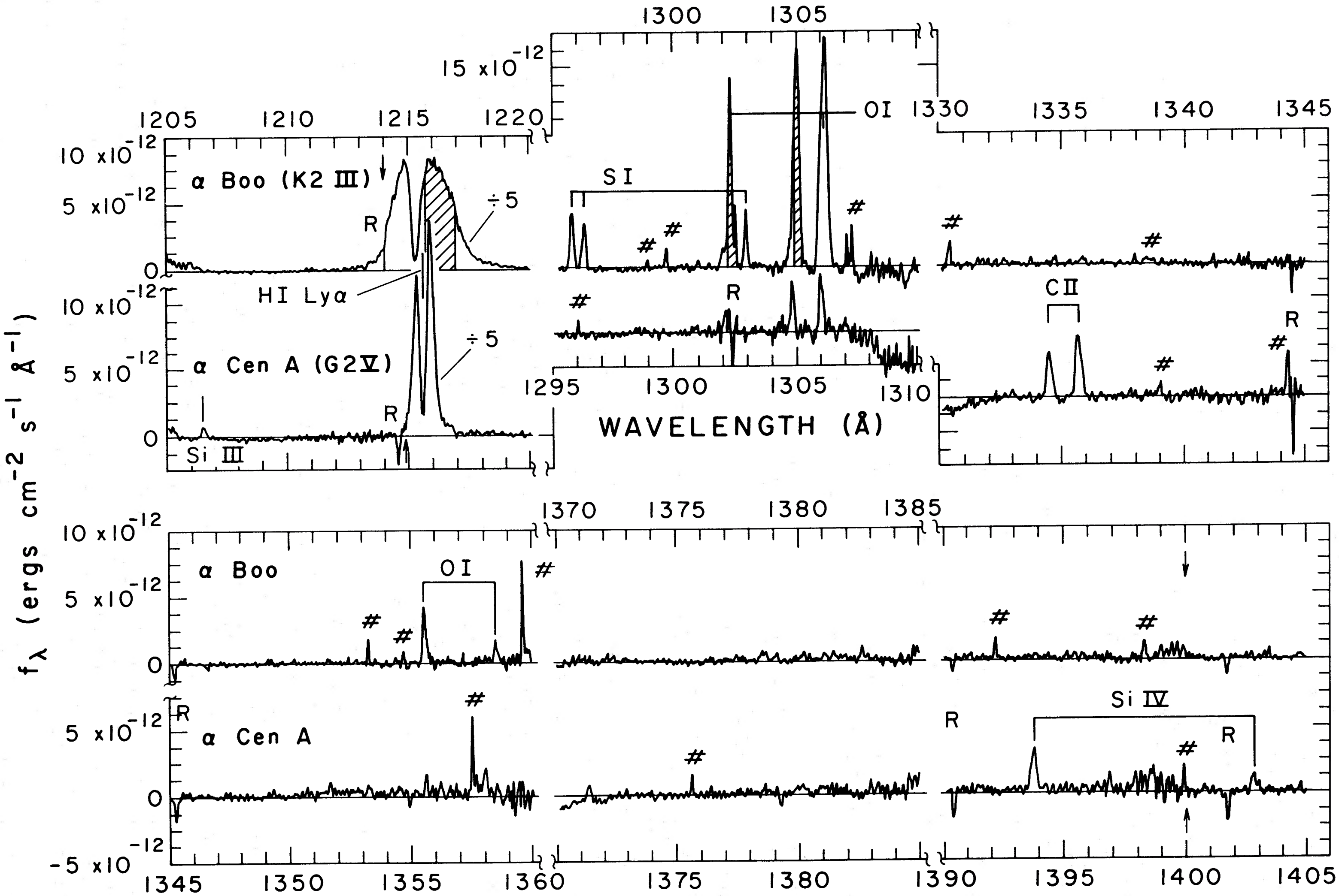

FIG. 1*a*.—Comparison of *IUE* far-ultraviolet emission spectra of the red giant Arcturus (α Boo; *top tracing in each panel*) and the yellow dwarf α Cen A (*bottom tracing*) from 1205 to 1405 Å. The ordinate of each panel is the monochromatic flux measured at Earth. The abscissa is a wavelength scale registered to the mean velocity of sharp emission features in each spectrum. Particular emission lines of interest are designed explicitly; R denotes reseau marks of the vidicon; # identifies particle radiation hits or blemishes (as determined from the photowrite representation of the echellogram); vertical arrows mark splice points between adjacent echelle orders; and cross-hatching indicates portions of the spectra affected by saturated pixels (or reseaux in some cases). Note that the bright H I Lyα λ1216 profiles of both stars have been scaled down by a factor of 5, and that the central region of the Arcturus Lyα absorption component is filled in partially by geocoronal emission. Also note that despite the strength of the Arcturus O I λ1305 triplet in apparent flux, the O I *surface* fluxes are about the same in both stars owing to the factor of 2.4 difference in angular diameters.

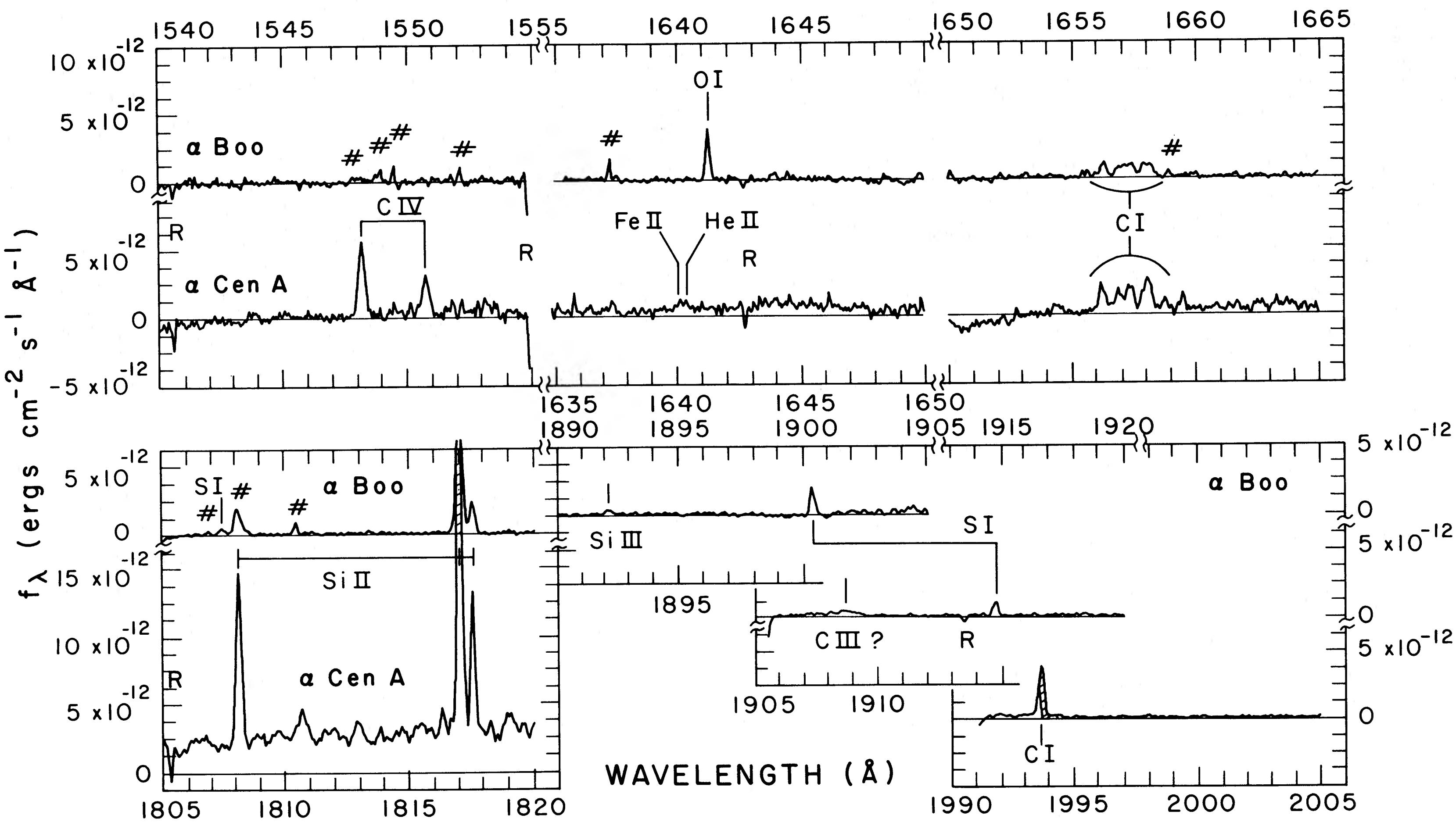

FIG. 1*b*.—Same as Fig. 1*a* for 1540–2005 Å. The *α* Cen A spectrum is not illustrated longward of 1820 Å owing to saturation of even the shortest exposure (120 minutes).

TABLE 3

Identifications and Line Shape Parameters

Identification	Laboratory Wavelength[a] (Å)	α Bootis (K2 III) V_L[b] (km s^{-1})	α Bootis FWHM (km s^{-1})	α Bootis $f_L \pm \sigma_G$[c] (10^{-12} ergs cm^{-2} s^{-1})	α Centauri A (G2 V) V_L[b] (km s^{-1})	α Centauri A FWHM (km s^{-1})	α Centauri A $f_L \pm \sigma_G$[c]
Soft X-rays	4–80	...	...	< 0.02(3 σ)	...	...	6
Si III	1206.510	...	...	...	−0	62	1.07±0.09
H I Lyα	1215.668	+1	550	[135±4][d]	+2	190	66±2[d]
N V	1238.821	...	...	< 0.3(3 σ)	+12	41	0.15±0.02
	42.804				+3	43	0.14±0.04
S I	1295.653	+2	42	0.78±0.01	...	...	...
	96.174	−6	49	0.68±0.07	...	...	...
O I	1302.169 }	+24	55	3.41±0.05	−1	62	0.55±0.04
S I	02.337 }						
S I	1302.863	−4	35	0.62±0.04	...	...	...
O I	1304.858	+23	71	5.01±0.31	−4	51	0.72±0.10
S I	05.883 }	+11	92	6.70±0.76	−7	34	0.74±0.03
O I	1306.029 }						
C II	1334.532	...	...	< 0.3(3 σ)	−2	52	0.85±0.11
	35.708				−1	65	1.43±0.08
Cl I	1351.657	...	...	...	−2	33	0.19±0.01
O I	1355.598	−3	29	0.57±0.02	−6	22	0.20±0.01
	58.512	+0	33	0.28±0.01	...	...	...
Si IV	1393.755	...	...	< 0.3(3 σ)	+3	56	0.92±0.07
	1402.770				+12	56	0.37±0.08
C IV	1548.185	...	...	< 0.3(3 σ)	+4	54	1.69±0.03
	1550.774				+1	56	0.94±0.04
C I	(1560)	...	...	...	...	...	(1.)
Fe II	1563.788	...	...	...	−5	52	0.32±0.04
Fe II	1640.150	...	...	...	−4	20	0.08±0.01:
He II	1640.400	...	...	< 0.1(3 σ)	−9	26	0.10±0.01
O I	1641.296	−5	33	0.75±0.01	...	...	...
Fe II	1654.476	...	...	...	−8	83	0.37±0.06
C I	1656.267	+7	71	0.41±0.06	−6	65	0.75±0.10
	56.928	...	...	... }	(−10)	(80)	(0.78±0.09)
	57.008	(+27)	(150)	(0.88±0.13) }			
	57.380	...	...	...	−6	65	0.88±0.07)
	57.907 }	(+3)	(90)	(0.58±0.08)	(+3)	(90)	(1.31±0.09)
	58.122 }						
Fe II	1658.771	...	...	...	−9	51	0.37±0.03
	59.483	...	...	...	−7	49	0.44±0.04
Fe II	1696.794	...	...	...	−1	57	0.48±0.05
S I	1807.310	+7	51	0.17±0.01	...	...	...
Si II	1808.012	+5	53	0.70±0.04	+5	41	3.10±0.09
	16.928	+1	45	2.52±0.10	−1	31	[7.30±0.03]
	17.451	−4	48	0.67±0.04	−1	31	2.28±0.07
S I	1820.343	+3	61	0.22±0.01	...	...	...
	26.245	+4	39	0.14±0.01	...	...	...
Si III]	1892.030	+9	59	0.18±0.01	...	...	...
S I	1900.286	+3	36	0.49±0.03	...	...	...
C III] ?	1908.734	−6:	91:	0.22±0.01:	...	...	...
S I	1914.698	+0	52	0.32±0.03	...	...	...
C I]	1993.620	+4	38	[0.90±0.08]	...	...	...
Mg II	2795.582	+3	90:	[266±20][e]	+5	83	203±13[e]
	2802.704	−3	84:	[211±20][e]	−5	95	172±13[e]

Note.—Brackets indicate saturate pixels included in fits. Parentheses indicate multiple features fitted as single feature.

[a] Kelly and Palumbo 1973.

[b] $\sigma_v \approx \pm 4$ km s^{-1} for both stars.

[c] In units of 10^{-12} ergs cm^{-2} s^{-1}. σ_G is obtained from rms deviation of measured profile from least squares Gaussian, and characterizes quality of fit. The *maximum* standard deviations of line fluxes derived from the rms fluctuations of featureless regions of the spectrum are $\sigma_s \cong 0.05$ (α Boo) and $\sigma_s \cong 0.06$ (α Cen A) for FWHM = 50 km s^{-1}. The *larger* of σ_G and σ_S is the appropriate measurement uncertainty. (Note, σ_s is somewhat smaller longward of 1800 Å where the SWP camera is most sensitive.)

[d] The Lyα profiles were fitted by Gaussians ignoring the lines cores, which are contaminated by interstellar absorption and geocoronal emission. The resulting fluxes are *upper limits* if the intrinsic stellar profiles have self reserved cores.

[e] Direct numerical integration of flux between k_1 (or h_1) features.

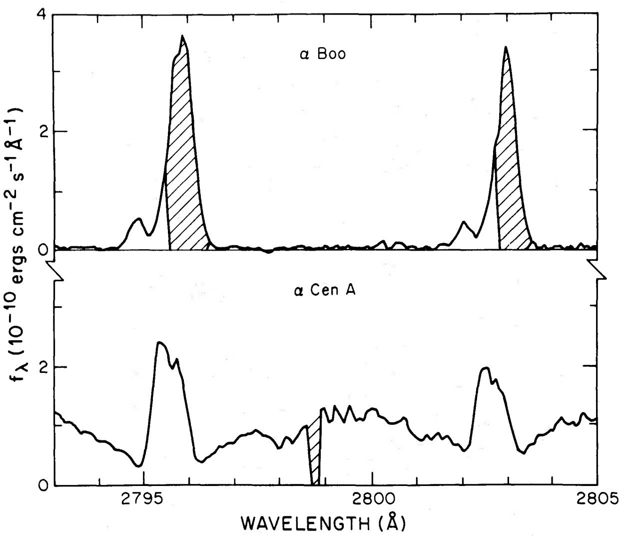

FIG. 2.—Mg II h and k features from the long-wavelength echellograms of Arcturus (*top panel*) and α Cen A (*bottom panel*). The Arcturus Mg II region was overexposed deliberately in order to investigate with good signal-to-noise the blueward distortions of the h and k profiles caused by wind expansion. Despite the apparent brightness of the Arcturus profiles, the Mg II *surface flux* is a factor of about 5 smaller than that of α Cen A.

ratio, $f_x/l_{\rm bol}$, and about 1500 times weaker in surface flux, F_x. At chromospheric temperatures ($T \approx 6 \times 10^3$ K), Arcturus is only a factor of 2 weaker than α Cen A in $f_{\rm Mg\ II}/l_{\rm bol}$ and a factor of 5 weaker in surface flux. The somewhat higher excitation ($T \approx 8 \times 10^3$ K) Si II $\lambda\lambda$1808, 1817 triplet appears to be weaker in Arcturus by perhaps a factor of 6 in $f_{\rm Si\ II}/l_{\rm bol}$ and nearly 20 in surface flux.

The highest excitation line that appears in the Arcturus spectrum is the λ1892 intersystem transition of Si III. (The α Cen spectrum is not illustrated in the region longward of 1820 Å because the photospheric continuum rises rapidly toward longer wavelengths and saturates even the 120 minute exposure.) The Si III] λ1892 flux, $1.8 \pm 0.3 \times 10^{-13}$ ergs cm^{-2} s^{-1}, is a factor of 3 smaller than that of the nearby S I λ1900 feature, which with S I λ1915 dominates the blend at 1900 Å seen in the low-dispersion spectrum of Arcturus (e.g., Ayres, Moos, and Linsky 1981).

If Si III] λ1892 is formed in a warm transition region (TR) above the chromosphere or in a 2×10^4 K chromospheric plateau (e.g., Simon, Kelch, and Linsky 1980), then we should expect to detect, at some level, permitted lines of similar excitation, namely C II $\lambda\lambda$1335, 1336. In giant stars for which both Si III] λ1892 and C II λ1336 are detected with certainty, the former is about twice as strong as the latter (Ayres *et al.* 1982). Accordingly, we would expect to detect C II λ1336 emission at a level of about 1×10^{-13}, which is somewhat smaller than the $3\ \sigma = 1.5 \times 10^{-13}$ upper limit if the width is comparable to that of C II in α Cen A (FWHM $\approx$ 65 km s^{-1}). Consequently, the absence of C II λ1336 emission at the sensitivity limits of the 7 hr *IUE* exposure does not rule out entirely a warm TR or a chromospheric plateau interpretation of the Si III] emission.

However, if a warm TR or chromospheric plateau were present in the outer atmosphere of Arcturus, it could occupy only a very small fraction of the plasma volume: the 3 σ upper limits on the C II $\lambda\lambda$1335, 1336 and C IV $\lambda\lambda$1548, 1551 surface fluxes are only 0.02 those of the quiet chromosphere dwarf comparison star, for which the surface filling fraction of bright TR structures presumably is quite small as in the solar case (cf. Withbroe and Noyes 1977). Furthermore, the absence of emission from the C II ($T \approx 2 \times 10^4$ K), Si IV (6×10^4 K), C IV (1×10^5 K) and N V (2×10^5 K) resonance lines probably also rules out the existence of a "warm" corona having a significant column emission measure, $\int n_e^2\, dh$, since the emission measure of a geometrically extended, nearly isothermal "corona" is much larger than that of a thermally contiguous "transition region" having the same base pressure (Gerola *et al.* 1974). For example, the column emission measure of the quiet Sun corona at $T \approx 10^6$ K exceeds that of the TR at C IV temperatures by more than an order of magnitude (Raymond and Doyle 1981). The Arcturus column emission measure at C IV is at least a factor of 50 smaller than that of α Cen A (or the quiet Sun). Accordingly, we probably can exclude any warm ($T \lesssim 10^5$ K) corona on Arcturus having a column emission measure greater than 0.002 that of the α Cen A (or the quiet Sun) corona.

If Arcturus possessed a corona at temperatures between 2×10^5 K and 10^6 K, we could not detect it spectroscopically in the far-ultraviolet or soft X-ray bands accessible to *IUE* or *Einstein*. However, the existence of material at temperatures exceeding 2×10^5 K surely would require conductive interfaces with the cooler chromospheric layers, and thereby produce some plasma at intermediate temperatures. Since the thermal interfaces seen in the Sun at C IV temperatures have approximately one-tenth the emission measure of the overlying hotter layers (the 10^6 K corona in that case), we probably can rule out a 2×10^5 K $\leq T \leq 1 \times 10^6$ K corona on Arcturus at column emission measures greater than 0.02 that of the quiet Sun (or α Cen A) corona.

Instead of a warm or hot corona, the outer atmosphere of Arcturus likely consists of an extended, low density, cool chromosphere. With the caveat that important collisional cross sections are uncertain, the ratio of the C II resonance line upper limit measured here to the *intersystem* C II UV 0.01 multiplet (2325 Å) line flux reported previously by Stencel *et al.* (1981) implies a temperature $T < 10^4$ K for the emitting region (cf. Brown, Ferraz, and Jordan 1980). Furthermore, ratios of components within the λ2325 multiplet and their individual emission measures indicate low densities ($n_e \approx 3 \times 10^8$) and highly extended geometries ($\Delta h \sim R_*$). If the emitting plasma is not much cooler than 10^4 K, it may be possible to explain the observed Si III intercombination line emission by collisional excitation of the few Si^{++} ions present. However, owing to the rapid decrease of the Si^{++} ionization fraction below 10^4 K, the low-temperature formation hypothesis for the Si III] feature must remain conjectural, pending a more definitive measurement for the temperature of the extended chromosphere of Arcturus.

b) The Cool Wind of Arcturus

The heavily distorted O I λλ1302, 1305 and Mg II *k* resonance line profiles of Arcturus depicted in Figure 3 indicate significant mass loss (cf. Chiu *et al.* 1977). (O I λ1306 is not illustrated in Fig. 3 owing to a blend with a fluoresced S I feature that masks the wind absorption profile.) Such a wind may play an important role in shedding angular momentum from an evolving solar mass star. We estimate the Arcturus mass loss rate as follows: The profiles of O I λλ1302, 1305 and Mg II *k* measured with *IUE* here and the *Copernicus* profile of Mg II *k* reported by McClintock *et al.* (1978) (also shown in Fig. 3) imply a wind terminal velocity of 40–50 km s^{-1}. The McClintock *et al.* analysis of the blueshifted absorption component in the high-resolution *Copernicus* profile indicates a Mg^+ column density of roughly 10^{15} cm^{-2} (McClintock *et al.* 1978). Assuming one-third solar abundances (Mäckle *et al.* 1975), and that all of the magnesium in the wind is Mg^+, we obtain a wind column mass density of about 2×10^{-4} g cm^{-2}. The corresponding mass loss rate for a spherically symmetric wind is:

$$\dot{\mathfrak{M}} = 4\pi r m v_\infty , \tag{1}$$

where v_∞ is the wind terminal velocity attained at a radial distance r, and m is the column mass density measured to that level. A lower limit to the mass loss rate, $\dot{\mathfrak{M}} \gtrsim 3\times10^{-10}\ M_\odot\ \mathrm{yr}^{-1}$, is obtained by assuming $r \approx R_*$, namely the wind accelerates rapidly to its terminal velocity just above the stellar photosphere. (A continued momentum deposition would, of course, be required to balance gravity.) The mass loss rate would be larger if the Mg^+ in the outermost regions of the wind is partially depleted by recombination (or the available magnesium reduced by grain formation), or if the terminal velocity is attained far from the star. The hydrogen number density at the base of the "minimum" wind is

$$n_\mathrm{H} \approx \frac{m}{1.4 m_\mathrm{H} R_*} \approx 5\times10^7\ \mathrm{cm}^{-3}. \tag{2}$$

This value is a factor of 6 smaller than the chromospheric *electron* density of 3×10^8 cm^{-3} estimated by Stencel *et al.* (1981) from the C II UV multiplet 0.01 line ratios. If the latter measurement actually refers to the wind itself, and if the plasma is largely ionized, then the mass loss rate could be increased to $\sim 2\times10^{-9}$ $M_\odot$ yr^{-1}. In contrast, Chiu *et al.* estimated $\dot{\mathfrak{M}} \approx 8\times10^{-9}$ $M_\odot$ yr^{-1} by simulating the asymmetric Ca II and Mg II profiles of Arcturus utilizing approximate radiative transfer calculations applied to a plane-parallel expanding atmosphere. More realistic calculations currently are under way for extended geometries in an effort to better estimate $\dot{\mathfrak{M}}$ from measured line asymmetries.

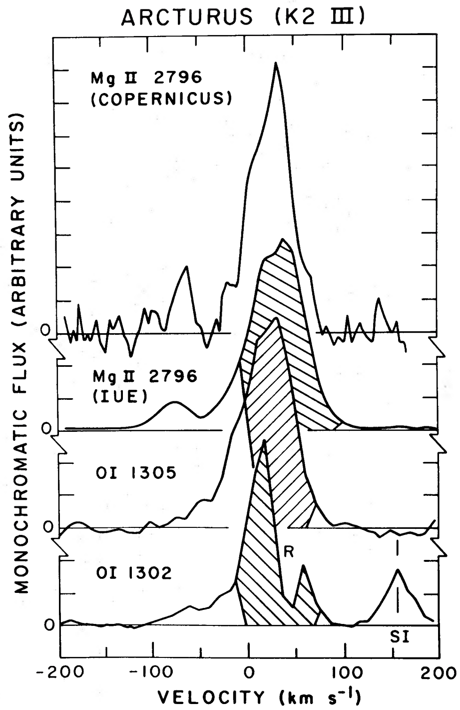

FIG. 3.—Comparison of O I λλ1302, 1305 and Mg II *k* emission profiles to illustrate effect of blueshifted wind absorption components. The uppermost Mg II *k* tracing is a high-resolution *Copernicus* profile as reported by McClintock *et al.* (1978). The wind terminal velocity is of order 40–50 km s^{-1}.

If the wind originates close to the stellar photosphere, the gravitational potential energy flux, $\sim mgv_\infty$, is 4×10^4 ergs cm^{-2} s^{-1} (expressed in equivalent surface flux units for $r = R_*$). The potential energy flux is an order of magnitude larger than the kinetic energy flux, $\sim \frac{1}{2} m R_*^{-1} v_\infty^3$. The total mechanical energy flux of the wind is an order of magnitude smaller than the surface radiative loss rate from the chromosphere in the H I, Mg II, and Ca II resonance lines of 3×10^5 ergs cm^{-2} s^{-1} (Ca II flux from Stencel *et al.* 1980). However, the wind nonradiative energy fluxes would be comparable to the "chromospheric" radiative loss rate if $\dot{\mathfrak{M}} \approx 2\times10^{-9}$ $M_\odot$ yr^{-1}.

Finally, the angular momentum flux for the Arcturus minimum wind is at least 10^4 times that of the solar wind, even though the Alfvénic moment arm of the solar wind (Durney 1972) is comparable to the photospheric radius of the red giant (25 $R_\odot$). The angular momentum loss rate of the Arcturus wind will increase another order of magnitude if $\dot{\mathfrak{M}}$ is as large as 2×10^{-9} $M_{\odot}$ yr^{-1}, or if the Arcturus wind also is coupled to its photosphere out to an Alfvén radius of several stellar radii.

The properties of the minimum mass flux wind derived here are similar to those of the Hartmann-MacGregor (1980) model 18, based on wind acceleration by Alfvén waves. The terminal velocity of the Arcturus wind appears to be somewhat lower, and the temperature maximum of the wind, $T_{\max} \leq 10^4$ K, is a factor of 2 or 3 smaller than predicted. These differences might be reconciled by reducing the wave damping length and initial wave flux in the theoretical model.

It is quite clear, however, that the Arcturus wind is not of the "hybrid" class proposed by Hartmann, Dupree, and Raymond (1980, 1981) for the yellow supergiants α Aqr (G2 Ib) and β Aqr (G0 Ib) and the red bright giant α TrA (K4 II). The authors suggest that the winds of the hybrid stars are warm ($T \approx 10^5$ K) close to the stars rather than cool ($T \approx 10^4$ K), owing to the presence of broad C IV emission lines in far-ultraviolet *IUE* spectra, in addition to blueshifted circumstellar absorption components in the Mg II lines. A class of the Hartmann-MacGregor models that incorporates large wave damping lengths can reproduce qualitatively some of the properties of the hypothesized warm winds of the hybrids (Hartmann, Dupree, and Raymond 1981).

However, we would like to propose an alternative interpretation of the "hybrid" wind of α TrA and by implication those of α Aqr and β Aqr as well. We believe that the broad C IV profiles observed in some G and K giants and supergiants are formed in optically thick active regions of closed magnetic geometry, while the remainder of the stellar surface is dominated by an open field geometry that permits significant mass flux in a cool wind similar to that of Arcturus. The diverging mass flow obscures the symmetric Mg II emission profiles from the magnetic active regions to produce the blueshifted absorption components. Our interpretation is based on the detection of broad C IV profiles in active chromosphere giants and supergiants like α Aur Ab (F9 III) and β Dra (G2 Ib) that show little or no evidence for circumstellar absorption (Ayres *et al.* 1982; Stencel *et al.* 1982) as well as in the hybrid star α TrA (Hartmann, Dupree and Raymond 1981) which does exhibit circumstellar absorption; the morphological similarity of the O I and Mg II profiles of α TrA and Arcturus; and the behavior of open and closed magnetic regions in the particularly well studied example of the Sun (Vaiana and Rosner 1978; Withbroe and Noyes 1977). We believe that the fundamental difference between (1) the active-chromosphere giants and supergiants, (2) the hybrid stars, and (3) the inactive red giants like Arcturus is in the fractional area of the stellar surface covered by active regions (compact bipolar magnetic structures) and "coronal holes" (open field geometry). The first group has the largest surface coverage of magnetic active regions, the second group has only a few active structures with increased "coronal hole" coverage to permit moderate winds, while the third group is dominated by open field regions and their winds, with only an occasional active area, if any at all.

We feel that an important strength of the Hartmann-MacGregor Alfvén wave–driven wind models is that the character of the mass loss changes dramatically from hot, low mass-flux winds among the high-gravity dwarfs and moderate-gravity yellow giants, to cool, large mass-flux winds among the low-gravity red giants and supergiants. Such an abrupt change is seen in spectroscopic indicators of cool winds within the giant branch itself (e.g., Stencel and Mullan 1980). However, we are concerned that a potential misinterpretation of C IV emission among the hybrid stars may cloud the true nature of their winds. The hybrid atmospheres of the supergiants in fact may be strongly bifurcated in a thermal sense: hot regions associated with closed magnetic structures, and a cool wind in open field regions. If so, the C IV features of α TrA (and α Aqr and β Aqr) tell us nothing concerning the physical state of its wind, in the same way that the spatially averaged X-ray flux of the Sun tells us nothing about the solar wind. Accordingly, we urge that the possibility of cool ($T \approx 10^4$ K) Alfvén wave–driven winds among such stars be investigated as an alternative to the warm wind models proposed previously.

c) *Line Shape Differences and the Wilson-Bappu Effect*

One of the striking differences between the far-ultraviolet spectra of Arcturus and α Cen A illustrated in Figures 1 and 2 is the large increase in line widths for the optically thick chromospheric features of the giant compared with the dwarf. For example, the base emission width of the Arcturus Mg II *k* line is about 1.7 times wider than that of α Cen A; Lyα is nearly 3 times broader in FWHM; and the Si II $\lambda\lambda$1808, 1817 triplet lines also are about 3 times broader (for an instrumental FWHM = 30 km s^{-1}) than *solar* profiles (FWHM $\approx$ 13 km s^{-1}; see Boland *et al.* 1975). The broadening of the chromospheric features in the red giant spectrum compared with that of the yellow dwarf is analogous to the width-luminosity behavior of the Ca II H and K emission cores discovered by Wilson and Bappu (1957). Two distinct explanations for the Wilson-Bappu effect have been proposed: (1) opacity broadening of a very opaque emission feature that is partially controlled by the Lorentzian wings of the profile function, and (2) broadening of an emission feature formed entirely within the Doppler dominated core of the profile function, induced by an increase in the atmospheric turbulence of giant stars relative to dwarfs (see Ayres 1979 and references therein). The high-resolution Arcturus spectrum reported here emphasizes the importance of the first mechanism.

In particular, we can estimate the nonthermal broadening in the chromospheric layers where Lyα and the Si II triplet are formed by considering the $\lambda\lambda$1808, 1817 widths. The triplet is optically thick in solar chromospheric models where the column mass density of material at Si II temperatures is only about 2×10^{-7} g cm^{-2} (Tripp, Athay, and Peterson 1978). In the Arcturus chromosphere, on the other hand, Si II emission can arise throughout an extended ($\Delta h \sim R_*$), low density ($n_e \lesssim 3\times10^8$ cm^{-3}) region that is not in hydrostatic equilibrium. If much of the region is partially ionized, the material column density of the red giant chromosphere might be as large as 1×10^{-3} g cm^{-2} in the layers that are warm enough to excite Si II emission (cf. Stencel *et al.* 1981). Although the actual excitation rate will be small owing to the reduced densities, the line center optical depths of the triplet features will be quite large ($\tau_{1c} \gtrsim 10^4$). Accordingly, the nonthermal velocity can be extracted from the heavily opacity broadened Doppler cores of the lines as follows (see, e.g., Ayres *et al.* 1982):

$$\xi \approx 0.6\ \mathrm{FWHM}\ (\ln \tau_{1c})^{-1/2}, \qquad (3)$$

where the last term is of order 1/3 for very opaque lines.

The measured mean width of the Si II triplet features in Arcturus is FWHM ≈ 36 km s^{-1} with the instrumental profile correction (assumed Gaussian). Applying equation (3) yields $\xi \approx 7$ km s^{-1}. The inferred nonthermal broadening is similar to that invoked to model solar Si II profiles (Tripp, Athay, and Peterson 1978), and clearly is much too small to explain the very large velocity widths of the Lyα and Mg II *h* and *k* features. Even if the Arcturus Si II triplet lines were optically thin, and consequently $\xi \approx 20$ km s^{-1}, the Lyα feature would still be broader than 10 local Doppler widths. Since the influence of the Doppler core of the profile function does not extend beyond about three Doppler widths from line center in an opaque transition (Mihalas 1978), the Lyα emission (as well as that of the Mg II doublet) must be controlled largely by the Lorentzian wings. Accordingly, the enhanced broadening of the resonance lines in the red giant spectrum must mostly be a response to the larger column densities of the extended, low-density chromosphere, rather than a result of increased turbulent motions in stars of low surface gravity (cf. Ayres 1979).

d) The Missing-Line Regions: CO *Fluorescence*

Ayres, Moos, and Linsky (1981) demonstrated that a number of features in the *IUE* low dispersion spectrum of Arcturus coincide with electronic bands of the carbon monoxide fourth positive system which can be pumped radiatively by strong chromospheric emission lines of O I (λ1305 triplet) and C I (λ1657 multiplet). In fact, the presence of fluoresced CO emission, particularly near λ1340 and λ1545, requires that we utilize high-dispersion spectra to set hard upper limits on the fluxes of C II $\lambda\lambda$1335, 1336 and C IV $\lambda\lambda$1548, 1551.

The fluoresced CO bands each consist of about 10 vibration-rotation lines concentrated within an interval of about 10 Å. Accordingly, we expect that their visibility will be enhanced at low dispersion (FWHM $\approx$ 6 Å) compared with the echelle spectra, where the individual features should be isolated and weak. That expectation is confirmed in Figure 1 by the absence of obvious features in the echelle orders centered near λ1340 and λ1380 of the Arcturus spectrum, while the intermediate region centered on λ1350 reveals prominent emission at λ1356 and λ1358 due to O I. (Note that the noise levels in each order are exaggerated toward the edges, indicated by arrows, owing to the echelle blaze correction.) In low-dispersion spectra, three features of comparable strength appear at λ1340, λ1360 and λ1380 (see Ayres, Marstad, and Linsky 1981; Ayres, Moos, and Linsky 1981). Clearly, higher sensitivity would be required to study in detail the vibration-rotation structure of the fluoresced CO bands. Future investigations of these features should provide important clues to the physical properties of the outermost, coolest layers of the red giant photosphere where the molecular concentration is maximum (cf. Brown *et al.* 1981).

IV. CONCLUSIONS

The high-resolution far-ultraviolet and soft X-ray studies of Arcturus and α Cen A reported here reinforce the conclusions of previous work that the hot coronae seen in solar mass dwarf stars suffer a dramatic decline in strength with evolution away from the main sequence. Although the surface fluxes of chromospheric indicators —Lyα, Mg II, and Si II—are factors of only 3 to 20 smaller in the red giant than in the quiet chromosphere dwarf, the surface flux of coronal soft X-ray emission is a factor of more than 1000 less in Arcturus than in α Cen A (or the Sun).

Accordingly, the rate of energy deposition to produce high temperature coronal material (as measured by F_x or f_x/l_{bol}) suffers as severe a decline over the comparatively brief evolutionary interval spent in the giant branch as over the entire main-sequence lifetime itself. The origin of the dramatic decay in coronal activity most likely is related to the rapid spin-down of the evolving star induced by expansion of its outer envelope and the development of a strong wind. The decrease in rotation is likely to inhibit the generation of magnetic flux by the dynamo mechanism (Parker 1970), or perhaps will simply not provide sufficient amplification of the field strength to permit the formation of the compact bipolar magnetic structures known to dominate coronal activity on the Sun (Vaiana and Rosner 1978).

Instead, we find on the red giant a highly extended chromosphere that expands slowly away from the star to form a cool wind of moderate mass flux. It is clear that the character of coronal magnetic fields on solar mass stars changes quite dramatically with evolution away from the main sequence.

On the other hand, the much milder decrease in chromospheric surface emission levels between the yellow dwarf and the red giant suggests that the heating of the lower atmosphere is less sensitive to evolutionary effects than the corona itself. Perhaps the fundamental mechanism is acoustic wave dissipation (see review by Ulmschneider 1979) that is augmented in the presence of magnetic fields, thereby accounting for the morphological association of bright chromospheric emission with compact magnetic structures seen clearly on the Sun. In fact, Arcturus may be an example of a "minimum flux" chromosphere for which the magnetic enhancement of acoustic energy deposition is very weak. Nevertheless, the chromosphere of the red giant still is comparatively bright, because the heating mechanism relies on a source of energy that is intimately associated with the surface bolometric energy flux (which is carried almost entirely by turbulent convection immediately beneath the stellar photosphere) rather than the magnetic field generation rate. However, the corona almost certainly requires the *in situ* dissipation of the magnetic field for its power source. In particular, the acoustic wave fluxes measured in the solar transition region at C IV temperatures are considerably smaller than the observed plasma energy losses of higher levels including the corona (Athay and White 1978, 1979; Bruner 1978). The sensitivity of the coronal heating mechanism to the detailed character of the embedded magnetic field can very likely account for the rapid disappearance of soft X-ray emission during the post–main-sequence evolution of solar mass stars.

In this regard, it is probable that the moderately strong stellar wind of Arcturus has played an important role in the spin-down of the star during its later evolutionary phases, since the lifetime in the core helium burning stage greatly exceeds the rather transient first and second ascents. However, the existence of such a wind poses a possible dilemma: If a low-mass red giant spends up to a billion years in the giant branch (Iben 1967) with a mass loss rate of as much as $10^{-9}\ M_{\odot}\ \mathrm{yr}^{-1}$, the mass *lost* may be comparable to the initial main sequence mass. Clearly, the evolution of a giant star would be affected by such a severe mass loss (cf. Dearborn, Kozlowski, and Schramm 1976). Perhaps the prolonged mass loss is the origin of the very low mass ($0.2\ M_{\odot}$) proposed for Arcturus by Mäckle *et al.* (1975), although their spectroscopic surface gravity analysis is controversial (see, e.g., Ayres and Johnson 1977).

Finally, an important issue raised by our analysis of Arcturus, which indicates a cool expanding chromosphere rather than a hot corona, is the character of mass loss in a low-mass red giant that is *still* magnetically active. Such giants should be found in close binaries ($P \lesssim 30^{\mathrm{d}}$) where the synchronization of rotational and orbital periods would maintain the fast rotation of the star in the face of evolutionary expansion and wind angular momentum loss. Are the winds of old, but active, red giants as strong as the Arcturus example? Or are the winds of active red giants inhibited simply by the decrease in open field regions imposed by the larger surface filling fraction of magnetically closed structures? Alternatively, the character of the dynamo might change entirely at some critical rotational velocity among the red giants (cf. Durney, Mihalas, and Robinson 1981). For example, fast rotating red giants in short-period binaries preferentially may produce strong fields of closed geometry, while the slowly rotating red giants may produce only weak fields of open geometry (that are conducive, however, to the acceleration of a cool wind by the Hartmann-MacGregor mechanism). The resolution of these issues must await detailed studies of the active red giants comparable to that we have undertaken here for Arcturus.

We thank Dr. A. Boggess and the Staff of the *IUE Observatory* for their help in the acquisition and reduction of the far ultraviolet spectra. We also thank Dr. F. Seward and the staff of the *Einstein* Guest Observer Program for their help in the acquisition and reduction of the soft X-ray image. This work was supported by the National Aeronautics and Space Administration through grants NAG5-199, NAG8-398, NAG5-82 and NGL-06-003-057 to the University of Colorado and NAG5-146 to the University of Hawaii.

REFERENCES

Athay, R. G., and White, O. R. 1978, *Ap. J.*, **226**, 1135.
______. 1979, *Ap. J. Suppl.*, **39**, 333.
Ayres, T. R. 1975, unpublished Ph.D. thesis, University of Colorado.
______. 1979, *Ap. J.*, **228**, 509.
______. 1980, in *The Universe at Ultraviolet Wavelengths: The First Two Years of IUE*, ed. R. D. Chapman (NASA Conf. Pub. 2171), p. 237.
Ayres, T. R., and Johnson, H. R. 1977, *Ap. J.*, **214**, 410.
Ayres, T. R., and Linsky, J. L. 1980, *Ap. J.*, **235**, 76.
Ayres, T. R., Linsky, J. L., Basri, G. S., Landsman, W., Henry, R. C., Moos, H. W., and Stencel, R. E. 1982, *Ap. J.*, **256**, 550.
Ayres, T. R., Linsky, J. L., Vaiana, G. S., Golub, L., and Rosner, R. 1981, *Ap. J.*, **250**, 293.
Ayres, T. R., Marstad, N. C. and Linsky, J. L. 1981, *Ap. J.*, **247**, 545.
Ayres, T. R., Moos, H. W., and Linsky, J. L. 1981, *Ap. J.* (*Letters*), **248**, L137.
Boesgaard, A. M., and Simon, T. 1981, in *Second Cambridge Workshop on Cool Stars, Stellar Systems, and the Sun*, ed. M. S. Giampapa and L. Golub (SAO Spec. Rept. 392, Vol. **2**, p.161).
Boggess, A., *et al.* 1978, *Nature*, **275**, 377.
Boland, B. C., *et al.* 1975, *M.N.R.A.S.*, **171**, 697.

Brown, A., Ferraz, M. C. de M., and Jordan, C. 1980, in *The Universe at Ultraviolet Wavelengths: The First Two Years of IUE*, ed. R. D. Chapman (NASA Conf. Publ. 2171), p. 297.
Brown, A., and Jordan, C. 1980, *M.N.R.A.S.*, **191**, 37P.
Brown, A., Jordan, C., Millar, T. J., Gondhalekar, P., and Wilson, R. 1981, *Nature*, **290**, 34.
Bruner, E. C., Jr. 1978, *Ap. J.*, **226**, 1140.
Caillault, J.-P., Helfand, D. J., and Ku, W. H.-M. 1981, *Bull AAS*, **13**, 811.
Cassatella, A., Ponz, D., and Selvelli, R. L. 1981, *IUE Newsletter*, No. 14, p. 270.
Chiu, H. Y., Adams, P. S., Linsky, J. L., Basri, G. S., Maran, S. P., and Hobbs, R. W. 1977, *Ap. J.*, **211**, 453.
Dearborn, D. S. P., Kozlowski, M., and Schramm, D. 1976, *Nature*, **261**, 210.
Duncan, D. K. 1981, *Ap. J.*, **248**, 651.
Durney, B. R. 1972, in *Solar Wind*, ed. C. P. Sonett, P. J. Coleman, Jr., and J. M. Wilcox (NASA SP-308), p. 282.
Durney, B. R., Mihalas, D., and Robinson, R. D. 1981, *Pub. A.S.P.*, **93**, 537.
Flannery, B. P., and Ayres, T. R. 1978, *Ap. J.*, **221**, 175.
Gerola, H., Linsky, J. L., Shine, R. A., McClintock, W., Henry, R. C., and Moos, H. W. 1974, *Ap. J. (Letters)*, **193**, L107.
Giacconi, R., *et al.* 1979, *Ap. J.*, **230**, 540.
Golub, L., Harnden, F. R., Jr., Pallavicini, R. Rosner, R., and Vaiana, G. S. 1982, *Ap. J.*, **253**, 242.
Griffin, R., and Griffin, R. 1967, *M.N.R.A.S.*, **137**, 253.
Hartmann, L., Dupree, A. K., and Raymond, J. C. 1980, *Ap. J. (Letters)*, **236**, L143.
______. 1981, *Ap. J.*, **246**, 193.
Hartmann, L., and MacGregor, K. B. 1980, *Ap. J.*, **242**, 260.
Iben, I., Jr. 1967, *Ann. Rev. Astr. Ap.*, **5**, 571.
Johnson, H. L., Mitchell, R. I., Iriarte, B., and Wisniewski, W. Z. 1966, *Commun. Lunar Planetary Lab.*, **4**, 99.
Kelly, R. L., and Palumbo, L. J. 1973, *Atomic and Ionic Emission Lines Below 2000 Angstroms* (NRL Report 7599).
Linsky, J. L., and Haisch, B. M. 1979, *Ap. J. (Letters)*, **229**, L27.
Linsky, J. L., Worden, S. P., McClintock, W., and Robertson, R. M. 1979, *Ap. J. Suppl.*, **41**, 47.
Mäckle, R., Griffin, R., Griffin, R., and Holweger, H. 1975, *Astr. Ap. Suppl.*, **19**, 303.
McClintock, W., Moos, H. W., Henry, R. C., Linsky, J. L., and Barker, E. S. 1978, *Ap. J. Suppl.*, **37**, 223.
Mihalas, D. 1978, *Stellar Atmospheres* (2d ed.; San Francisco: Freeman).
Parker, E. N. 1970, *Ann. Rev. Astr. Ap.*, **8**, 1.
Raymond, J. C., and Doyle, J. G. 1981, *Ap. J.*, **245**, 1141.
Simon, T., Kelch, W. L., and Linsky, J. L. 1980, *Ap. J.*, **237**, 72.
Simon, T., Linsky, J. L., and Stencel, R. E. 1982, *Ap. J.*, **257**, 225.
Skumanich, A. 1972, *Ap. J.*, **171**, 565.
Skumanich, A., Smythe, C., and Frazier, E. N. 1975, *Ap. J.*, **200**, 747.
Stencel, R. E., Linsky, J. L., Ayres, T. R., Jordan, C., and Brown, A. 1982, *Ap. J.*, submitted.
Stencel, R. E., Linsky, J. L., Jordan, C., Brown, A., Carpenter, K. G., Wing, R. F., and Czyzak, S. 1981, *M.N.R.A.S.*, **196**, 47P.
Stencel, R. E., and Mullan, D. J. 1980, *Ap. J.*, **238**, 221.
Stencel, R. E., Mullan, D. J., Linsky, J. L., Basri, G. S., and Worden, S. P. 1980, *Ap. J. Suppl.*, **44**, 383.
Stern, R. A., Zolcinski, M.-C., Antiochos, S. K., and Underwood, J. H. 1981, *Ap. J.*, **249**, 647.
Thomas, J. A., Hyland, A. R., and Robinson, G. 1973, *M.N.R.A.S.*, **165**, 201.
Tripp, D. A., Athay, R. G., and Peterson, V. L. 1978, *Ap. J.*, **220**, 314.
Ulmschneider, P. 1979, *Space Sci. Rev.*, **24**, 71.
Vaiana, G. S., and Rosner, R. 1978, *Ann. Rev. Astr. Ap.*, **16**, 393.
Wilson, O. C. 1963, *Ap. J.*, **138**, 832.
Wilson, O. C., and Bappu, M. K. V. 1957, *Ap. J.*, **125**, 661.
Withbroe, G. L., and Noyes, R. W. 1977, *Ann. Rev. Astr. Ap.*, **15**, 363.

THOMAS R. AYRES: Laboratory for Atmospheric and Space Physics, University of Colorado, Boulder, CO 80309

JEFFREY L. LINSKY: Joint Institute for Laboratory Astrophysics, University of Colorado, Boulder, CO 80309

THEODORE SIMON: Institute for Astronomy, University of Hawaii, Honolulu, HI 96822